Chapter-4

Exploration of Auxochromic Effects of Alicyclic Amines on Coumarin Fluorophore

4. Exploration of Auxochromic Effects of Alicyclic Amines on Coumarin Fluorophore

4.1. Background and Rationale

In the previous chapter, we examined the role of annulated azacoumarins as potential fluorophores and discovered dihydropyrrolo-4-methylcoumarin to possess all the desired photophysical and physicochemical properties, along with a free nitrogen centre for attaching a response unit in developing a fluorescent probe. As a result, we investigated its use in designing and synthesizing a peroxide-detecting probe (**PYCB**) for sensitive and specific monitoring of changes in cellular peroxide levels.

The potential benefits of these annulated azacyclic auxochromes are vast. However, their application outside the coumarin core is currently limited by challenges in their synthetic feasibility and the availability of suitable starting materials. As a result, the adaptability of these auxochromes is constrained, which restricts their integration with other fluorescent moieties. We actively pursued a more versatile auxochrome that possesses all the necessary features and can be seamlessly integrated into other fluorophore cores to generate exceptionally bright dye molecules.

As mentioned earlier, 7-hydroxy-4-methyl coumarin (**1**) has been widely used as fluorescent organic molecules owing to their well-established photophysical properties and good cell permeability.[1] The electron-donating hydroxyl group in the 7-position is crucial for fluorescence emission of **1** (figure 4.1). The replacement of the hydroxyl group with an amine at the 7-position resulted in 7-amino-4-methylcoumarin (**2,** figure 4.1), which exhibits a fairly high quantum yield ($\Phi_f = 0.5$).[2] Simple alkylation of **2** to diethylamino analogue (**3**) leads to a bathochromic shift in their absorption and fluorescence emission wavelengths accompanied by a large decrease in the quantum yield (figure 4.1). Coumarin-based fluorescent molecules normally exhibit excited state intramolecular charge transfer (ESICT), but in the presence of a tertiary amine substituent at the 7th position (as in the case of **3**), the rate of population of

twisted intramolecular charge transfer (TICT) is enhanced that subsequently quenches the fluorescence of the entire molecule by non-radiative relaxation. Due to their fluorescence properties, compound **3** offers advantages for *in vivo* imaging, but lesser quantum yield somewhat restricts their use.[1,3] Azetidine-substituted fluorophores (as in the case of **4**, figure 4.1) were found to demonstrate larger bathochromic shift and quantum yields of fluorescence as compared to diethylamino (**3**) counterparts. [4,5] Aziridine-substituted fluorophores (**5**) were also found to behave similarly.[6] The introduction of azetidine or aziridine substitution suppresses the occurrence of TICT which subsequently improves the fluorescence brightness of these types of molecules.

Our objective was to find a versatile auxochrome that can be integrated into any fluorophore and possess a centre for the attachment of response units without sacrificing the desired fluorogenic properties of previously discovered advanced amino-based auxochromes. Thus, we introduced *N*-cycloalkylamines onto the 7-position of 4-methyl coumarin (target molecules, figure 4.1) and compare their photophysical properties with standard **4**. The target molecules could be synthetically accessed by Buchwald-Hartwig coupling.

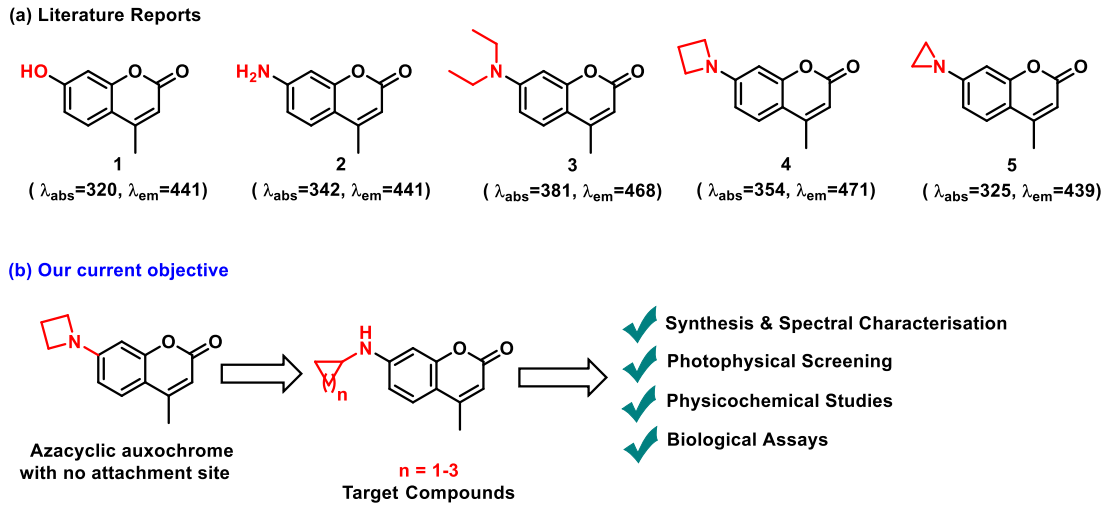

Figure 4.1. (a) Previous work depicting fluorescent coumarin analogues containing electron-donating hydroxy (**1**), amino (**2**), diethylamino (**3**), azetidine (**4**), and aziridine (**5**) rings as

reported in the literature and (b) current work objective depicting incorporation of cycloalkylamines as auxochromes at the 7th position of 4-methylcoumarin to synthesize target molecules.

4.2. Results and Discussion

4.2.1. Synthesis of desired compounds

Due to a lack of suitable syntheses of halogenated coumarins,[7] the commercially available **1** was converted to corresponding triflate **1a** by treatment with trifluoromethane sulfonic anhydride in pyridine at -10 °C for 3 h (scheme 4.1). The intermediate **1a** thus obtained was then subjected to Buchwald-Hartwig amination with cyclopropyl amine using $Pd_2(dba)_3$, xantphos and Cs_2CO_3 as base in dioxane at 100 °C for 12 h for the synthesis of 4-methyl-7-cyclopropylamino coumarin (**6**). Compound **6** was obtained in 19% yield. The O-S bond in triflate **1a** was found to be unstable and cleaved to give the saponified product **1** (method A). The use of TBAF·$3H_2O$ as an additive in the above condition suppressed the triflate saponification (method B) [6] and improved the yield of product **6** (45%), but the de-triflated product **1b** prevailed as a major issue.

Scheme 4.1. Synthesis of 4-methyl-7-cyclopropylamino coumarin (6) using 4-methyl umbelliferone-7-triflate (1a) as intermediate.

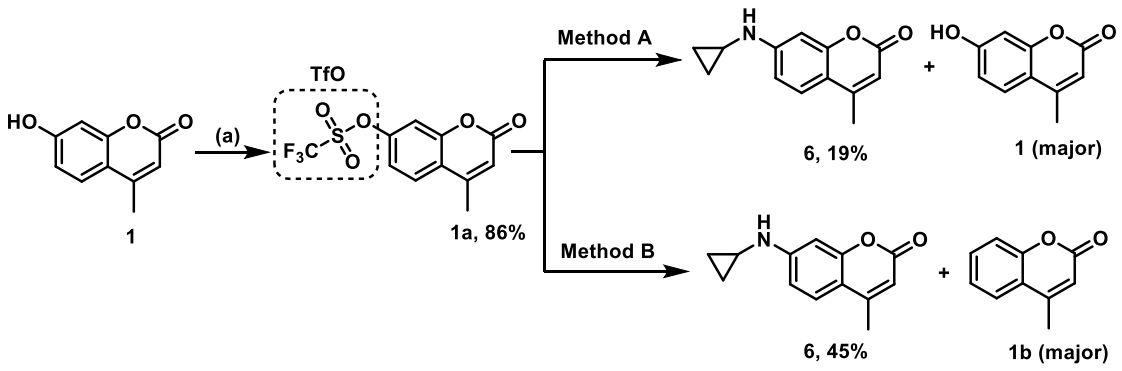

Reagents and conditions: (a) **1** (1 eq.), Tf_2O (2.5 eq.), pyridine (1.5 eq.), acetonitrile, -10 °C, 2 h; (b) Method A: **1a** (1 eq.), Cyclopropylamine (2 eq.), $Pd_2(dba)_3$ (5 mol%), Xantphos (10 mol%), Cs_2CO_3 (2 eq.), 1,4-Dioxane, 100 °C, 12 h. Method B: Same as Method A in the presence of TBAF·$3H_2O$ (1 eq.).

In order to circumvent the instability and saponification problems of triflate, we have synthesized a nonaflate derivative of compound **1**. It has been reported that the nonaflates are less prone to O-S bond cleavage than corresponding triflates which subsequently causes the hydrolysis.[8,9] Besides, the strong electron-withdrawing perfluorinated butyl chain with SO_2 moiety enhances the reactivity of nonaflates by acting as a good leaving group.[10,11] The 4-methyl-7-nonafluorobutylsulfonyloxy coumarin intermediate **1a'** was synthesized by the reaction of **1** with perfluorobutanesulfonyl fluoride (PBSF), K_2CO_3 in acetonitrile at room temperature for 4 h (scheme 4.2). Further, we treated the intermediate **1a'** with cyclopropylamine, $Pd_2(dba)_3$/xantphos combinations and Cs_2CO_3 as base in dioxane at 100 °C for 12 h. To our delight, we have observed that product **6** was obtained in better yield (72%, table 4.1, entry 1) but hydrolysed compound **1** still remained as a side-product. Fortunately, the addition of TBAF·$3H_2O$ (1 equiv.) significantly reduced the hydrolysis of the nonaflate and product **6** was obtained in acceptable yield (scheme 4.2, entry 2). We have used various $Pd_2(dba)_3$/ligand combinations (table 4.1, entry 3-5), but the best result was obtained in $Pd_2(dba)_3$/xantphos combination (table 4.1, entry 2). The use of other solvents like toluene, DMF, and NMP resulted in compound **6** in 60%, 46% and 35% yields, respectively (table 4.1, entry 6-8). Among the various bases screened (table 4.1, entries 2, 9 and 10), Cs_2CO_3 gave the best yield of product **6**.

Scheme 4.2. Synthesis of 4-methyl-7-cyclopropylamino coumarin (6) using 4-methyl umbelliferone-7-nonaflate (1a') as intermediate.[a]

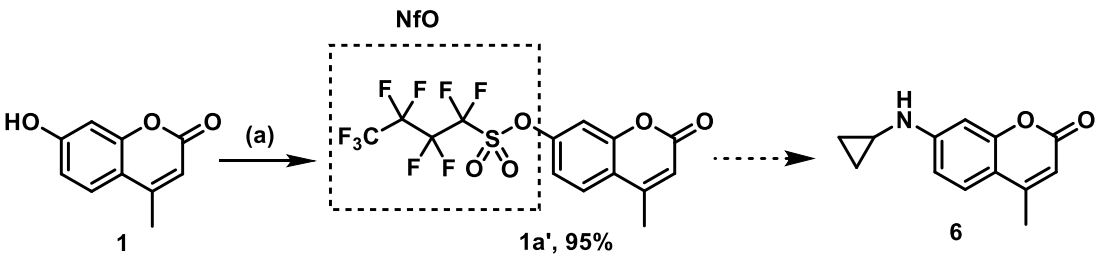

[a]**Reagents and Conditions.** (a) **1** (1 mmol), Perfluorobutanesulfonylfluoride (PBSF) (1 eq.), K_2CO_3 (1.5 eq.), acetonitrile, rt, 2 h.

Table 4.1. Optimization conditions of reaction for synthesis of compound 6 from intermediate 1a'.[b]

Entry	Catalyst	Ligand	Base	Additive	Solvent	Yield 6 (%)[c]
1	$Pd_2(dba)_3$	Xantphos	Cs_2CO_3	-	Dioxane	72
2	$Pd_2(dba)_3$	Xantphos	Cs_2CO_3	TBAF·$3H_2O$	Dioxane	86
3	$Pd_2(dba)_3$	BINAP	Cs_2CO_3	TBAF·$3H_2O$	Dioxane	54
4	$Pd_2(dba)_3$	dppf	Cs_2CO_3	TBAF·$3H_2O$	Dioxane	Traces
5	$Pd_2(dba)_3$	Xphos	Cs_2CO_3	TBAF·$3H_2O$	Dioxane	48
6	$Pd_2(dba)_3$	Xantphos	Cs_2CO_3	TBAF·$3H_2O$	Toluene	60
7	$Pd_2(dba)_3$	Xantphos	Cs_2CO_3	TBAF·$3H_2O$	DMF	46
8	$Pd_2(dba)_3$	Xantphos	Cs_2CO_3	TBAF·$3H_2O$	NMP	35
9	$Pd_2(dba)_3$	Xantphos	K_2CO_3	TBAF·$3H_2O$	Dioxane	32
10	$Pd_2(dba)_3$	Xantphos	K*t*OBu	TBAF·$3H_2O$	Dioxane	Traces

[b]**Reagents and conditions**: **1a'** (1 mmol), cyclopropyl amine (2 mmol), $Pd_2(dba)_3$ (5 mol%), ligand (10 mol%), base (2 mmol), TBAF·$3H_2O$ (1 mmol), solvent (4 ml), 100 °C, 12 h. [c]Isolated yield.

Buoyed by the success of this approach, we then sought access to entire classes of 7-cyclic alkylamino modifications heretofore unknown in umbelliferone analogues. Buchwald–Hartwig amination with xantphos allowed ready access to a wide variety of 7-cycloalkylamino derivatives (scheme 4.3, compounds **6-9**). Furthermore, primary and secondary 7-alkylamine analogues could also be synthesized directly in good yields under these conditions (scheme 3, compounds **10-18**). Azetidine and pyrrolidine analogues were similarly accessed with palladium-catalyzed amination using xantphos as a ligand (scheme 4.3, compounds **4** and **19**).

Thus, this family of compounds are readily accessible by operationally simple Buchwald-Hartwig protocol. We also checked the robustness of the method by carrying out a large-scale amplification experiment of **1a'** (2.3 g, 5 mol) under optimized reaction conditions, which smoothly gave compound **8** in 82% yield (scheme 4.4).

Scheme 4.3. Substrate scope of various amines for Buchwald-Hartwig coupling with 1a'.[a]

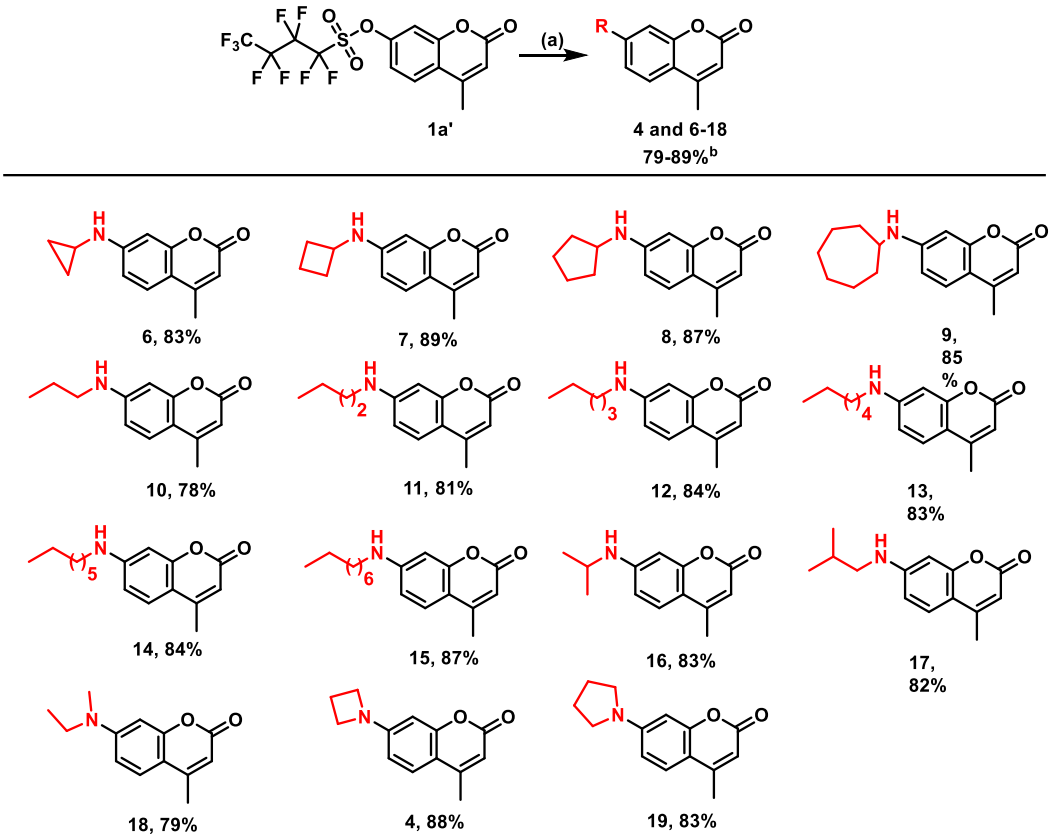

[a]**Reagents and conditions**: **5** (1 mmol), various amines (2 mmol), $Pd_2(dba)_3$ (5 mol%), xantphos (10 mol%), Cs_2CO_3 (2 mmol), TBAF·$3H_2O$ (1 mmol), solvent (4 ml), 100 °C, 12 h. [b]Isolated yields.

Scheme 4.4. Gram scale synthesis of compound 8.[a]

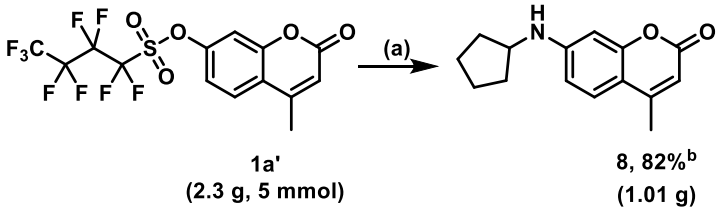

[a]**Reagents and conditions**: **1a'** (2.3 g, 5 mmol), cyclopentylamine (2.43 g, 10 mmol), $Pd_2(dba)_3$ (229 mg, 0.25 mmol), xantphos (289 mg, 0.50 mmol), Cs_2CO_3 (3.2 g, 10 mmol), TBAF·$3H_2O$ (1.3 g, 5 mmol), solvent (20 ml), 100 °C, 12h. [b]Isolated yield.

4.2.2. Photophysical Characterization of Molecules

The fluorescence emission wavelengths (figure 4.2) and intensity of compounds **6-19** were evaluated in phosphate buffer solution (PBS 1X) and compared with compound **4**. The fluorescence emission peaks for compounds **6**, **7**, **8** and **9** were 462, 468, 469, and 462 nm, respectively (figure 4.2a). As the size of *N*-cycloalkylated substitution grows, emission wavelength increases but interestingly, there is a sudden dip in emission wavelength for the cycloheptylamine (**9**). Mono- and di-substituted alkyl amines (compounds **10-18**) showed emission wavelength in the range of 466-470 nm (figure 4.2b). Larger cyclic amine, pyrrolidinyl substituted compound **19** displayed emission wavelength at 476 nm. None of the compounds showed better emission wavelength compared to **4** (478 nm).

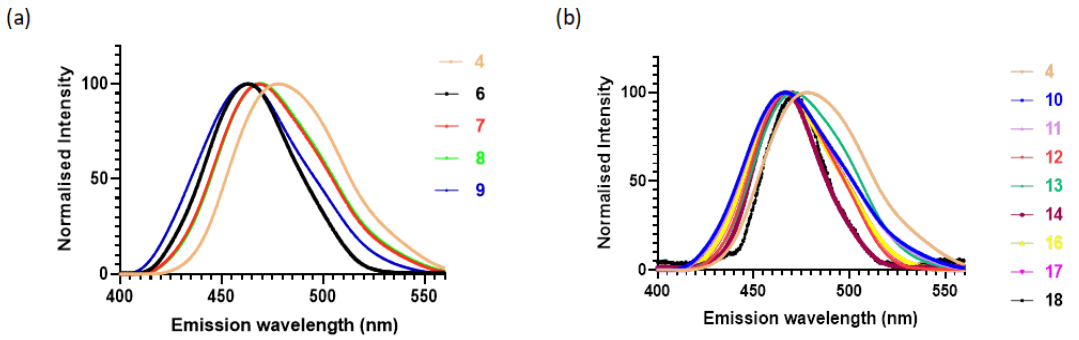

Figure 4.2. (a) Fluorescence emission peaks for compounds **6-9** in comparison with **4**. (b) Mono- and di-substituted alkyl amine (compounds **10-18**) emission wavelength in comparison with **4.**

Absolute quantum yields (ϕ_f) of the compounds were calculated in presence of an integrating sphere and are noted below in table 4.2. In cycloalkylamine derivatives **6-9**, the increase in ring size resulted in the increase of light-emitting properties**.** Cyclobutyl derivative **7** ($\phi_f \approx 0.952$)

and cyclopentyl derivative **8** ($\phi_f \approx 0.963$) showed greater quantum yields as compared to cyclopropyl substituted **6** ($\phi \approx 0.054$). Further increase in the ring size to cycloheptyl in compound **9** ($\phi_f \approx 0.641$) resulted in a decrease in the light emission, possibly reflecting the flexibility in the ring system. A similar trend was observed in straight-chain alkyl substitutions (**10-15**). *n*-Butyl substituted **11** ($\phi_f \approx 0.940$) showed greater quantum yield compared to *n*-propyl substituted **10** ($\phi_f \approx 0.752$). Further increase in the length of the alkyl chain (**12-15**) showed a gradual decrease in quantum yield. Compounds **16** ($\phi_f \approx 0.930$) and **17** ($\phi_f \approx 0.950$) with branched chain alkyl group showed high quantum yield compared to **10** and **11** with straight chain alkyl group with same number of carbon atoms. Compound **18** with ethylmethylamine substitution displays a low quantum yield ($\phi_f \approx 0.020$). Azetidinyl-substituted coumarin such as **4** ($\phi_f \approx 0.935$) displays larger quantum yields of fluorescence (ϕ_F) compared to pyrrolidinyl substituted **19** ($\phi \approx 0.732$). This improvement in ϕ_f values has been attributed to a decrease in the rate of population of TICT states. This high quantum yields **11** and **17** can be attributed to the presence of larger hydrophobic groups attached to the amino group that effectively reduces the hydrogen bonding with water and helps to protect the fluorescence. However, since the water solubility of these analogues gets diminished owing to the enhanced hydrophobicity, they were not further carried on for cell imaging as solubility issues may arise.

Table 4.2. Photophysical properties of compounds **4** and **6-19** in PBS.

Comp. no.	λ_{abs} (nm)[a]	λ_{em} (nm)[b]	Stokes' Shift (nm)	ε[c] (M^{-1} cm^{-1})	ϕ_f[d]	Brightness (M^{-1} cm^{-1})
6	363	462	99	-	0.054	-
7	360	468	108	8700	0.952	8282
8	355	469	114	11600	0.963	11179
9	370	462	92	7200	0.641	4616
10	362	466	104	32600	0.752	24525
11	340	467	127	13500	0.940	12691

12	360	467	107	20110	0.651	13091
13	365	470	105	20060	0.297	5960
14	372	467	95	-	0.050	-
15	359	467	108	-	0.044	-
16	365	466	101	71100	0.930	66137
17	362	467	105	19800	0.950	18812
18	370	470	100	-	0.020	-
19	378	476	98	8600	0.732	6295
4	355	478	123	12100	0.935	11320

[a]λ_{abs} = absorbance maximum in PBS; [b]λ_{em} = emission maximum in PBS; [c]Molar absorptivity in PBS; [d]Quantum yield in PBS.

4.2.3. Theoretical explanation of findings using DFT studies

In order to examine the impact of cycloalkylamines on coumarin dyes, quantum chemical studies were conducted on compounds 6-9 using DFT/B3LYP 6-31++G(d,p) and TD-DFT/B3LYP 6-31++G(d,p) methods via Gaussian 09 software. The results were then compared with those of standard **4**. Theoretical calculations revealed the excited state (S_1) geometrical conformations of compounds **4** and **6-9** (as depicted in figure 4.3b-4.3c). Based on the literature, the high quantum yield of **4** (Φ_f= 0.96) can be attributed to the uninterrupted electron flow owing to the coplanarity of azetidine to the coumarin, along with the structural rigidity and resistance to TICT. Upon replacing azetidine with a cyclopropylamine as an electron donor in compound **6**, the loss of planarity and increase in ring strain might account for the sudden decrease in quantum yield. Additionally, the increase in ring size to cyclobutyl and cyclopentyl (compounds **7** and **8**, respectively) led to a restoration of quantum yields due to reduced ring strain and a somewhat planar conformation of the ring systems. However, increasing to a cycloheptylamine ring resulted in a loss of brightness due to structural distortion of the ring and deviation from planarity.

The electronic distributions of compounds **6-9**, and their respective HOMO and LUMO energy gaps (figure 4.3d) illustrate that the electron density of the HOMO of all the compounds is uniformly delocalized on the coumarin scaffold and the amine moiety, predominantly on the nitrogen atom and the adjacent two carbon atoms. In the LUMO, the electron density on the amine rings of **6-9** shifts completely towards the lactonic portion of the coumarin core, showcasing the push-pull effect on the D-π-A system of the established fluorophore. The shorter HOMO-LUMO energy band gap in compound **4** (3.71 eV) corresponds to a longer emission wavelength (λ_{em} = 478 nm), whereas a significant increase in the band gap (3.94 eV) in compound **6** can be the rationale behind the blue shift of the emission maximum (λ_{em} = 462 nm). A consistent trend of a slightly high energy gap in compounds **7** and **8** (3.84 eV and 3.82 eV, respectively) can be attributed to their slightly blue-shifted emission maxima (λ_{em} = 468 and 469 nm, respectively). Again, a higher HOMO-LUMO gap in compound **9** (3.94 eV) leads to a lower emission wavelength (λ_{em} = 468 nm).

To the best of our knowledge, azetidinyl group have been widely used to increase the quantum yield of coumarins. However, we have demonstrated that subtle auxochrome structure variation leads to the enhancement of fluorescence properties. As observed, the incorporation of cyclobutylamine and cyclopentylamine in place of azetidine can also elevate the fluorogenic properties of a fluorophore and help retain its brightness.

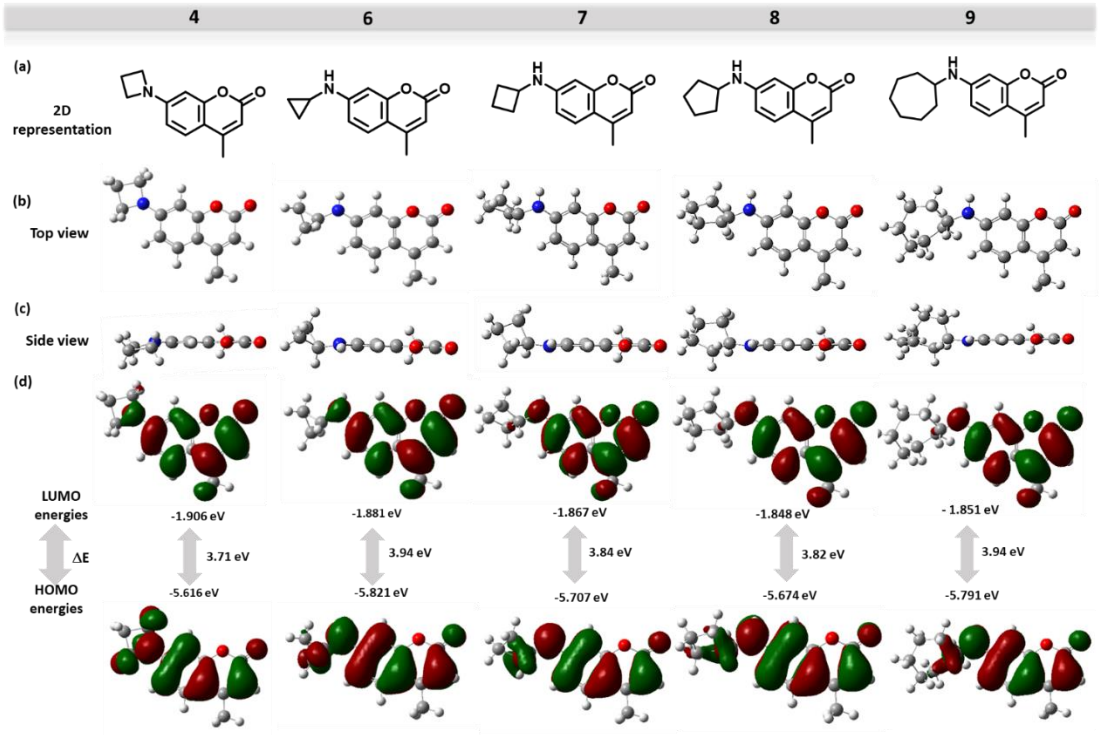

Figure 4.3. Illustrations of (a) 2D chemical structure, (b) top view and (c) side view of excited state geometries (S_1) and (d) HOMO (highest occupied molecular orbital) and LUMO (lowest unoccupied molecular orbital) electron densities of compounds **4** and **6-9** in water using TD-DFT/B3LYP 6-31++g(d, p) method along with the IEFPCM model of Gaussian 09 software.

4.2.4. pH Stability and Photostability Studies of molecules

Delighted with their excellent photophysical properties, compounds **7** and **8** were further subjected to assessment of their pH stability and photostability. Compounds **7** and **8** showed no significant changes in their fluorescence emission intensity and exhibited substantial stability (figure 4.4a-b) over the physiological pH range (4-8). Evaluation of the photostability of compounds **7** and **8** was conducted in comparison to azetidinylated counterpart **4** by a time-dependent photobleaching method using coumarin **6** (λ_{ex}: 457 nm; λ_{em}: 501 nm) as the reference dye (figure 4.4c-d). The results of this test indicated that compounds **7** and **8** remain photostable over a substantial period of 6 h, and their stability to white light irradiation was somewhat comparable to that of the azetidinylated derivative **4** (figure 3.3b).

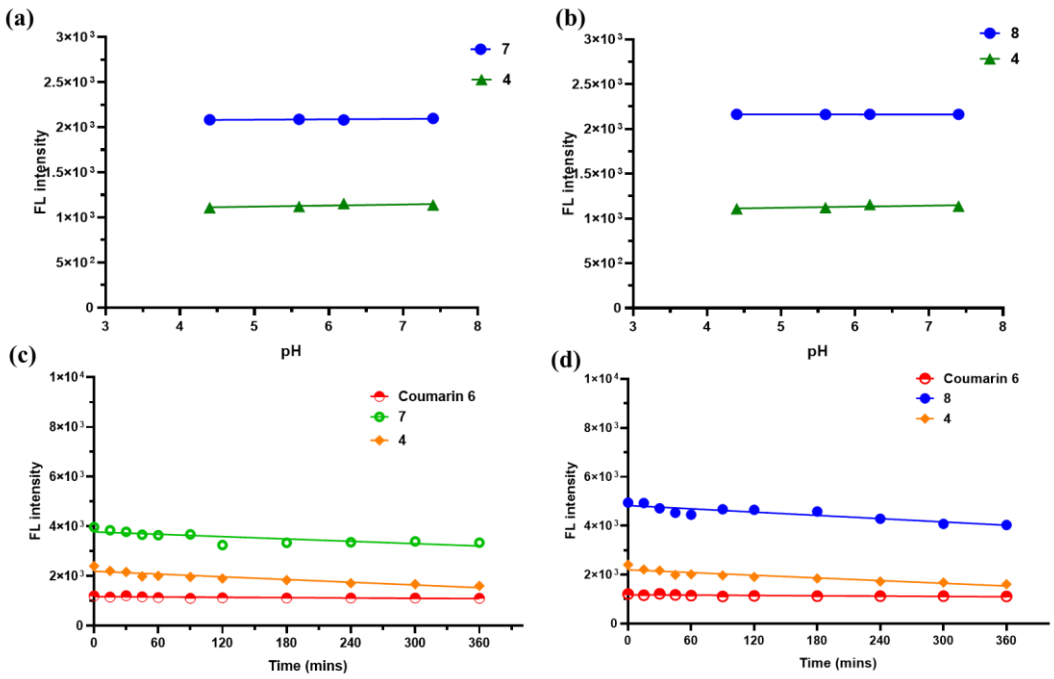

Figure 4.4. (a, b) Evaluation of the stability of compounds **7** and **8** in response to pH as compared to their reference standard **4**, respectively; (c, d) Photostability tests of compounds 7 and 8 in comparison to standard **4,** respectively using coumarin 6 as the reference dye.

4.2.5. Biocompatibility Assay, Cellular Uptake and Fluorescence Imaging Studies on Molecules

Finally, we investigated the potential applications of dyes **4**, **7** and **8** in cellular imaging. Prior to bioimaging, the cytotoxicity of dyes **4**, **7** and **8** were determined by MTT assays on both MDA-MB-231 breast cancer cell line as well as non-cancerous HEK-293 human epidermal kidney cell lines. MTT assay in MDA-MB-231 cells (figure 4.5a) demonstrated that there was no significant cytotoxicity on the tested cell line, even at a higher concentration of 100 µM than the concentration used for bioimaging. However, in normal HEK-293 cells (figure 4.5b), compounds **7** and **8** showed slight cytotoxicity at higher concentrations (beyond 50 µM), but these were comparatively biosafe than standard **4** at all possible concentrations. Further, the cellular uptake of compounds **4**, **7** and **8** by the living cells was explored by fluorescence

microscope after an incubation for 12 h. The images were captured in green and blue channels, which were then merged with phase contrast. The obtained images (figure 4.6) depict fair uptake of the compounds **4**, **7** and **8** by the cancer cells and are in fact, distributed thoroughly throughout the cells. The fluorescence emission intensities of the compounds after cancer cell uptake were further quantitatively measured by using flow cytometry (figure 4.7). It is noted that the average fluorescence intensity exhibited by the cell population treated with compound **7** was much higher as compared to that of the standard **4** (figure 4.8). However, compound 8 showed somewhat poor cellular permeability. These results indicated that these dyes can stain the cells well with negligible cytotoxicity and demonstrate that cycloalkylamine-substituted coumarins can be well used in biological imaging.

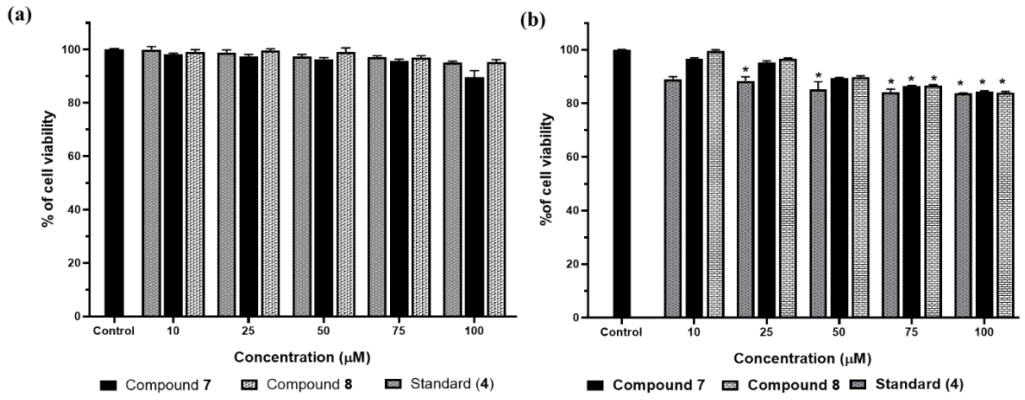

Figure 4.5. Measurement of percentage of viability of (a) MDA-MB-231 cancer cells and (b) HEK-293 normal cells incubated with compounds **4, 7** and **8** at various concentrations ranging from 10 μM to 100 μM for 24 h. Statistical analysis has been done by one-way ANOVA followed by Tukey's test where * denotes a significant difference ($p<0.05$).

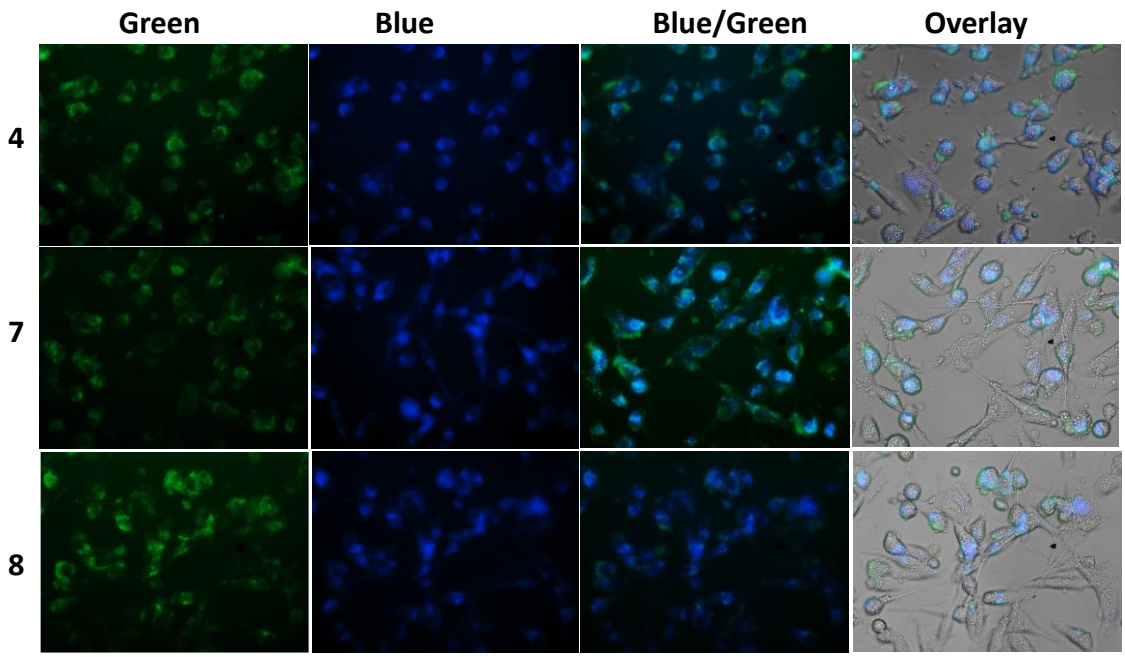

Figure 4.6. Fluorescence images of MDA-MB-231 cells after incubation with dyes **4**, **7** and **8** at a concentration of 75 μM for 12 h at 37 ºC.

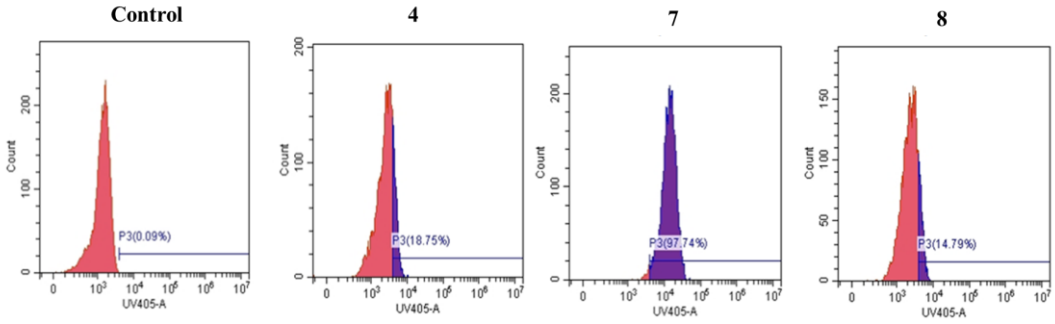

Figure 4.7. The fluorescence intensity of compounds **4**, **7**, and **8** were determined through flow cytometry against MDA-MB-231 cell lines after 30 min of incubation.

4.3. Conclusion

In conclusion, we have expanded the scope of luminogenic coumarins beyond the canonical azetidine analogue by synthesizing 7-cycloalkylaminocoumarins using Buchwald-Hartwig cross coupling reactions. The scope of the reaction extends to a variety of substrates such as cycloalkylamines, alkylamines, and cyclic amines in good to excellent yields. The photophysical properties of synthesized analogues revealed that compounds **7** and **8** have the

highest quantum yields, slightly elevated than standard compound **4**. Theoretical analysis suggests that the ring size of cycloalkylamine plays a drastic role in controlling the brightness of the coumarin scaffolds. Further evaluations show decent pH stability and photostability of these compounds. MTT assay in MDA-MB-231 cell lines depicts excellent biocompatibility of both compounds **7** and **8**. Fluorescence imaging in MDA-MB-231 cell lines further demonstrates the future scope of application of such new dyes in *in vivo* imaging. Cycloalkylamines, especially cyclobutylamine and cyclopentylamine, show all the perks of azetidine auxochrome and also provide a nitrogen centre for further functionalization into a biochemical-detecting probe.

4.4. Experimental Section

4.4.1. Materials and Methods

All chemicals were purchased from Sigma-Aldrich, TCI Chemicals, SRL Chemicals, and Avra, and used as received. Molychem silica gel (60-120 mesh) was used for column chromatography, and thin-layer chromatography was performed on Merck pre-coated silica gel 60-F254 plates. All other chemicals and solvents were obtained from commercial sources and purified using standard methods. The characteristic FTIR spectra of the functional groups present in the synthesized molecules were obtained using Bruker Alpha ATR instrument. The ^{1}H NMR and ^{13}C NMR spectra were recorded on Bruker-Advance 500 and 600 MHz spectrometers. Chemical shifts (δ) are reported in parts per million (ppm), using TMS (δ = 0) as an internal standard and $CDCl_3$ and d^6-DMSO as NMR solvents. The mass spectrum of the compounds has been obtained by Waters Q-ToF Premier Mass Spectrometer. UV absorbance was measured on Agilent Cary UV 60 UV-Visible Spectrophotometer. Fluorescence data were recorded on a Molecular Devices SpectraMax M5 multimode plate reader. Solvent used for fluorescence spectra: Dichloromethane (DCM), Methanol (MeOH) and PBS, 1X (SRL

Chemicals). GraphPad Prism ver. 7.0a (GraphPad Software, Inc.) was used to analyze data and generate graphs.

4.4.2. Photophysical Characterization

UV absorbance was measured on Agilent Cary UV 60 UV-Visible Spectrophotometer. Molar absorption coefficients (ε) were determined by direct application of Beer−Lambert's law using solutions of compounds **4** to **19** (except **18**) in PBS (1X) with concentrations ranging from 10^{-6} to 10^{-5} M. Fluorescence data were recorded on a Horiba Scientific FluoroMax-4. The solvent used for measuring fluorescence spectra: PBS, 1X (SRL Chemicals). GraphPad Prism ver. 7.0a (GraphPad Software, Inc.) was used to analyze data and generate graphs.

4.4.3. Absolute Quantum Yield Measurement

Absorbance spectra were recorded for each sample at a single concentration with an absorbance ranging between 0.07-0.09. The absolute quantum yields (QYs) of the synthesized compounds were obtained with the use of a PTI K – Sphere petite Integrating sphere and quantum yield calculations were done through Horiba PTI Fluorescence Quanta Master 400 Systems. For evaluating the quantum yield of different sample, the quartz cuvette located at the centre of the integrating sphere filled with different sample solutions (in 1X PBS) to ensure the maximum interaction of light with the sample regardless of its direction or angle. The integrating sphere allows the collection of all the light emitted and scattered by the fluorescent sample. Samples were excited with different excitations with the help of 75 W Xe PTI arc lamp housing (A-1010B).

4.4.4. Computational Studies

Computational studies were performed with the help of Gaussian 09 software. Density functional theory (DFT) and time-dependent (TD)-DFT calculations were used to measure the

spectral properties of compounds **6-9** using their azetidinyl counterpart (**4**) as the reference. Geometry optimizations for **4** and **6-9** in the ground state (S_0) and in the first excited singlet state (S_1) were carried out employing the B3LYP functional with the 6-31++G(d,p) basis set. Energy minimum after ground state (S_0) geometry optimizations were ensured by frequency calculations. Solvent effects (water) were taken into consideration using the IEFPCM model. Evaluations of DFT and TD-DFT theory used to calculate the absorption and emission maxima along with the energy gap between S_0 and S_1 states are found to be in good agreement with the practically obtained spectroscopic data.

4.4.5. pH Stability and Photostability Studies

For the pH stability study, the buffers having pH ranges 4-8 were prepared using deionized water following standard protocol and freshly used. Compound **4, 7** and **8** in a fixed concentration was placed in each buffer system and incubated for 30 mins at 37 ^{o}C before measuring the fluorescence intensities. For photostability tests, the compounds **4, 7**, **8** and standard **coumarin 6** were dissolved in DMSO:PBS mixture in a volume ratio of 20:80 in separate vials and placed under continuous irradiation with a 500W tungsten lamp emitting white light. Their emission intensities were then measured after 0, 15, 30, 45, 60, 90, 120, 180, 240 and 360 minutes of irradiation and the obtained fluorescence intensities were plotted into a curve against time.

4.4.6. Cell culture and conditions

The breast cancer cell line (MDA-MB-231) was procured from the National Centre for Cell Science (NCCS), Pune, India. DMEM (Dulbecco's Modified Eagle Medium**)** and 12 well cell culture plates were purchased from Genetix Private Limited. The 96 well plates and T-25 flasks were purchased from Eppendorf. Penicillin-streptomycin, Trypsin-EDTA, and FBS (Fetal Bovine Serum) were purchased from Gibco. PBS (Phosphate Buffer Saline) was prepared in

the laboratory. The MDA-MB-231 cells were cultured in DMEM, supplemented with FBS and penicillin-streptomycin solution and grown in a humidified CO_2 incubator at 37 °C.

4.4.7. *In vitro* Cytotoxicity assay

For analysis of the cytotoxicity of the compounds (**4**, **7** and **8**) against the MDA-MB-231 cell line, cells were seeded in the density of 10,000 cells per well on a 96-well cell culture plate followed by overnight incubation to allow the adherence of the cells. After 24 hours of incubation of the cells with different concentrations of the synthesized compounds (10 µM, 25µM, 50 µM, 75 µM and 100 µM), the media from each well was aspirated and replaced with fresh media comprising of MTT-containing solution. The MTT-containing media was removed after 2 hours of incubation, followed by addition of 100 µl of DMSO in each well and incubation for another 30 minutes. The absorbance was determined at 570 nm using a multiplate reader.

4.4.8. Intracellular uptake studies in cells and evaluation of light emission at different time intervals

Intracellular uptake study was performed in MDA-MB-231 cell lines. Cells were seeded at the density of 0.5 x 10^5 cells per well in a 12-well plate, followed by overnight incubation for allowing the adherence of the cells. The cells were then treated with a 75 µM concentration of each treatment and then incubated for 12 hours. Prior to imaging, the media were aspirated, washed with chilled PBS, and images were captured *via* phase contrast microscope (400 X magnification) as well as fluorescence using blue and green channels with a 3s exposure.

4.4.9. Synthesis and characterization of compounds

4.4.9.1. Synthesis of 4-Methyl-2-oxo-2H-chromen-7-yl trifluoromethanesulfonate (1a)

7-hydroxy-4-methylcoumarin (1 g, 5.6 mmol) was added to a flame-dried flask. The solid was suspended in acetonitrile (14 mL), and pyridine (0.9 mL, 11.3 mmol) was added. The suspension was cooled to -10 °C. A solution of trifluoromethanesulfonic anhydride (1.91 g, 6.7 mmol, 1.1 mL) in dry acetonitrile (3 mL) was added dropwise. The mixture was stirred for 30 min at –10 °C, then reaction was stirred for further 30 min at room temperature. The solution was washed twice with 0.1 M HCl, followed by H_2O and brine. The organic phase was dried over Na_2SO_4 and the solvent was removed under reduced pressure. The product was purified by column chromatography in 20% ethylacetate/hexane to yield 1.1 g (63% yield) of **1a** as an off-white solid. Spectral data match with literature reported value.

4.4.9.2. Synthesis of 7-(cyclopropylamino)-4-methyl-2H-chromen-2-one (6) from 1a

Method A: A round bottom flask was charged with **1a** (308 mg, 1 mmol), cyclopropylamine (114 mg, 2 mmol), tris(dibenzylideneacetone)palladium (46 mg, 0.05 mmol), xantphos (57 mg, 0.10 mmol), caesium carbonate (652 mg, 2 mmol) and dioxane (4.0 mL) under argon. The resulting solution was heated at 100 °C with rapid stirring for 12h. The reaction mixture was allowed to cool to room temperature and then diluted with water (20 mL) and extracted with ethyl acetate (25 mL ×3). After drying with anhydrous Na_2SO_4, the organic phase was evaporated to dryness and purified by column chromatography using 30% ethyl acetate: hexane as eluent to yield **6** (40 mg, 19% yield) as an orange solid.

Method B: A round bottom flask was charged with **1a** (308 mg, 1 mmol), cyclopropylamine (114 mg, 2 mmol), tris(dibenzylideneacetone)palladium (46 mg, 0.05 mmol), xantphos (57 mg, 0.10 mmol), caesium carbonate (652 mg, 2 mmol), TBAF.$3H_2O$ (279 mg, 1 mmol), and dioxane (4.0 mL) under argon. The resulting solution was heated at 100 °C with rapid stirring for 12h.

The reaction mixture was allowed to cool to room temperature and then diluted with water (20 mL) and extracted with ethyl acetate (25 mL ×3). After drying with anhydrous Na_2SO_4, the organic phase was evaporated to dryness and purified by column chromatography using 30% ethyl acetate: hexane as eluent to yield **6** (95 mg, 45% yield) as an orange solid.

4.4.9.3. Synthesis of 4-methyl-7-nonafluorobutylsulfonyloxy coumarin (1a')

Reaction of 7-hydroxy-4-methylcoumarin (2 g, 11.2 mmol) with perfluorobutanesulfonyl fluoride (PBSF) (4.05g, 13.4 mmol) and K_2CO_3 (8.5 mmol, 1.5 equiv.) in acetonitrile at room temperature for 4 h allows complete conversion and precipitation of **1** from solution. The reaction mixture was then diluted with H_2O and extracted with ethyl acetate (3 x 20 ml). The combined organic layer was dried with anhydrous sodium sulphate, concentrated *in vacuo* and purified by column chromatography to afford the pure product **1** in excellent yield (95%) as an easy-to-handle white crystalline powder with extended periods of chemical stability.

4.4.9.4. General Procedure for Synthesis of Compounds 6-19 and 4 from 1a'

A round bottom flask was charged with **1a'** (1 mmol), various amines (2 mmol), tris(dibenzylideneacetone)palladium (5 mol %), xantphos (10 mol %), caesium carbonate (2 mmol), TBAF.$3H_2O$ (1 mmol), and dioxane (4.0 mL) under argon. The resulting solution was heated at 100 °C with rapid stirring for 12h. The reaction mixture was allowed to cool to room temperature and then diluted with water (20 mL) and extracted with ethyl acetate (25 mL ×3). After drying with anhydrous Na_2SO_4, the organic phase was evaporated to dryness and purified by column chromatography using ethyl acetate: hexane.

4.4.9.5. Gram scale synthesis of compound 8.

A round bottom flask was charged with **1a'** (2.3 g, 5 mmol), cyclopropylamine (0.84 g, 10 mmol), tris(dibenzylideneacetone)palladium (229 mg, 0.25 mmol, xantphos (289 mg, 0.50 mmol), caesium carbonate (3.2 g, 10 mmol), TBAF.$3H_2O$ (1.3 g, 5 mmol), and dioxane (20.0

mL) under argon. The resulting solution was heated at 100 ºC with rapid stirring for 12 h. The reaction mixture was allowed to cool to room temperature and then diluted with water (50 mL) and extracted with ethyl acetate (50 mL × 3). After drying with anhydrous Na_2SO_4, the organic phase was evaporated to dryness and purified by column chromatography using ethyl acetate: hexane.

4.4.9.6. Spectral Data of Synthesized Compounds

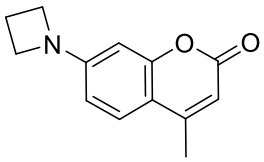

7-(azetidin-1-yl)-4-methyl-*2H*-chromen-2-one (4): The representative general procedure mentioned above was followed. The compound was purified by column chromatography using 20% ethyl acetate:hexane. Compound **4** was obtained as a brownish yellow solid with 88% yield. ^{1}H NMR (600 MHz, $CDCl_3$) δ 7.39 (d, *J* = 8.4 Hz, 1H), 6.32 (dd, *J* = 2.4 Hz, 1.8 Hz, 1H), 6.23 (d, *J* = 1.8 Hz, 1H), 5.99 (s, 1H), 4.01 (t, *J* = 7.2 Hz, 4H), 2.48 - 2.43 (m, 2H), 2.36 (s, 3H). ^{13}C NMR (150 MHz, $CDCl_3$) δ 162.0, 155.6, 154.0, 153.0, 125.4, 110.3, 109.4, 107.7, 97.1, 51.8, 18.6, 16.5. HRMS (ESI) m/z calculated for $C_{13}H_{13}O_2N$ $[M + H]^+$ calculated as 216.1019, found 216.1039.

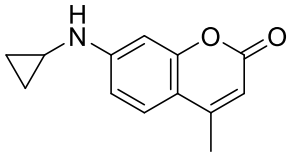

7-(cyclopropylamino)-4-methyl-*2H*-chromen-2-one (6): The representative general procedure mentioned above was followed. The compound was purified by column chromatography using 30% ethyl acetate:hexane. Compound **6** was obtained as an orange solid with 83% yield. ^{1}H NMR (600 MHz, $CDCl_3$) δ 7.37 (d, *J* = 9.0 Hz, 1H), 6.74 (d, *J* = 1.8 Hz,

1H), 6.64 (dd, *J* = 1.8 Hz, 2.4 Hz, 1H), 6.01 (s, 1H), 4.72 (s, 1H), 2.52 - 2.50 (m, 1H), 2.36 (s, 3H), 0.83 - 0.82 (m, 2H), 0.58 - 0.57 (m, 2H). ^{13}C NMR (150 MHz, $CDCl_3$) δ 162.0, 155.7, 153.1, 152.1, 125.3, 110.9, 110.6, 109.6, 99.0, 24.8, 18.6, 7.6. HRMS (ESI) m/z calculated for $C_{13}H_{13}O_2N$ $[M + H]^+$ calculated as 216.1019, found 216.1039.

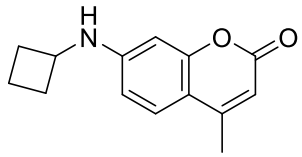

7-(cyclobutylamino)-4-methyl-*2H*-chromen-2-one (7): The representative general procedure mentioned above was followed. The compound was purified by column chromatography using 30% ethyl acetate:hexane. Compound **3d** was obtained as a greenish yellow solid with 89% yield. ^{1}H NMR (600 MHz, $CDCl_3$) δ 7.32 (d, *J* = 9 Hz, 1H), 6.47 (dd, *J* = 2.4 Hz, 2.4 Hz, 1H), 6.38 (d, *J* = 1.8 Hz, 1H), 5.95 (s, 1H), 4.68 (s, 1H), 3.96 - 3.91 (m, 1H), 2.47 - 2.42 (m, 2H), 2.32 (s, 3H), 1.91-1.80 (m, 4H). ^{13}C NMR (150 MHz, $CDCl_3$) δ 162.2, 155.9, 153.2, 150.5, 125.5, 110.5, 110.4, 109.1, 98.2, 48.4, 30.8, 18.6, 15.3. HRMS (ESI) m/z calculated for $C_{14}H_{15}O_2N$ $[M + H]^+$ calculated as 230.1176, found 230.1197.

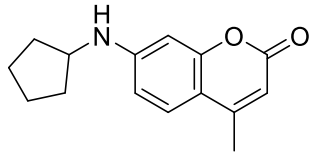

7-(cyclopentylamino)-4-methyl-*2H*-chromen-2-one (8): The representative general procedure mentioned above was followed. The compound was purified by column chromatography using 35% ethyl acetate:hexane. Compound **8** was obtained as a brownish yellow solid with 87% yield. ^{1}H NMR (600 MHz, $CDCl_3$) δ 7.26 (s, 1H), 6.42 - 6.38 (m, 2H), 5.87 (s, 1H), 4.34 (s, 1H), 3.74 (s, 1H), 2.25 (s, 3H), 1.99 (s, 2H), 1.67 - 1.59 (m, 4H), 1.45 (s, 1H). ^{13}C NMR (151 MHz, $CDCl_3$) δ 162.2, 155.9, 153.2, 153.1, 151.3, 125.4, 110.7, 110.1,

108.9, 98.3, 54.4, 33.3, 24.1, 18.6. HRMS (ESI) m/z calculated for $C_{15}H_{17}O_2N$ $[M + H]^+$ calculated as 244.1332, found 244.1361.

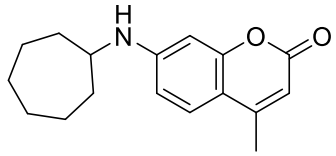

7-(cycloheptylamino)-4-methyl-*2H*-chromen-2-one (9): The representative general procedure mentioned above was followed. The compound was purified by column chromatography using 30% ethyl acetate:hexane. Compound **9** was obtained as a whitish yellow solid with 85% yield. ^{1}H NMR (500 MHz, $CDCl_3$) δ 7.35 (d, *J* = 9.0 Hz, 1H), 6.46 (dd, *J* = 2.5 Hz, 2.0 Hz, 1H), 6.39 (d, *J* = 2.5 Hz, 1H), 5.98 (d, *J* = 1.0 Hz, 1H), 4.19 (d, *J* = 6.0 Hz, 1H), 3.52 - 3.49 (m, 1H), 2.35 (s, 3H), 1.71 - 1.50 (m, 12H). ^{13}C NMR (125 MHz, $CDCl_3$) δ 162.1, 156.1, 152.9, 150.5, 125.5, 110.8, 110.1, 109.1, 98.3, 53.7, 34.6, 28.1, 24.3, 18.5. HRMS (ESI) m/z calculated for $C_{17}H_{21}O_2N$ $[M + H]^+$ calculated as 272.1645, found 272.1671.

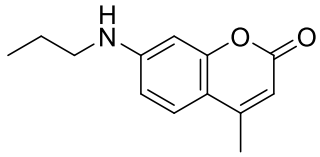

4-methyl-7-(propylamino)-*2H*-chromen-2-one (10): The representative general procedure mentioned above was followed. The compound was purified by column chromatography using 40% ethyl acetate:hexane. Compound **10** was obtained as a yellowish-brown solid with 78% yield. ^{1}H NMR (500 MHz, $CDCl_3$) δ 7.35 (d, *J* = 8.75 Hz, 1H), 6.51 (dd, *J* = 2 Hz, 2.5 Hz, 1H), 6.45 (d, *J* = 2.5 Hz, 1H), 5.97 (s, 1H), 4.29 (s, 1H), 3.15 (q, *J* = 7 Hz, 2H), 2.35 (s, 3H), 1.72-1.65 (m, 2H), 1.02 (t, *J* = 7 Hz, 3H). ^{13}C NMR (126 MHz, $CDCl_3$) δ 162.0, 156.0, 153.0, 151.7, 125.4, 110.3, 110.2, 109.2, 97.9, 45.2, 22.3, 18.5, 11.5. HRMS (ESI) m/z calculated for $C_{13}H_{15}O_2N$ $[M + H]^+$ calculated as 217.1103, found 217.1093.

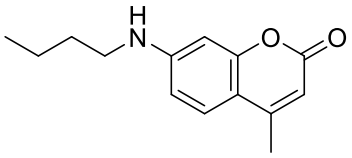

4-methyl-7-(butylamino)-*2H*-chromen-2-one (11): The representative general procedure mentioned above was followed. The compound was purified by column chromatography using 40% ethyl acetate:hexane. Compound **11** was obtained as a dark green solid with 81% yield. ^{1}H NMR (500 MHz, $CDCl_3$) δ 7.36 (d, *J* = 8.5 Hz, 1H), 6.51 (dd, *J* = 2 Hz, 2.5 Hz, 1H), 6.46 (d, *J* = 2.5 Hz, 1H), 5.99 (s, 1H), 4.20 (s, 1H), 3.19 (t, *J* = 7.0 Hz, 2H), 2.36 (s, 3H), 1.67 - 1.62 (m, 2H), 1.50 - 1.42 (m, 2H), 0.99 (t, *J* = 7.5 Hz, 3H). ^{13}C NMR (126 MHz, $CDCl_3$) δ 162.1, 156.0, 153.0, 151.7, 125.4, 110.4, 110.2, 109.3, 97.9, 43.2, 31.2, 20.2, 18.5, 13.8. HRMS (ESI) m/z calculated for $C_{14}H_{17}O_2N$ $[M + H]^+$ calculated as 232.1332, found 232.1320.

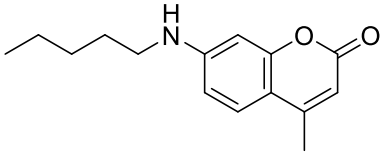

4-methyl-7-(pentylamino)-*2H*-chromen-2-one (12): The representative general procedure mentioned above was followed. The compound was purified by column chromatography using 40% ethyl acetate:hexane. Compound **12** was obtained as a brownish yellow solid with 84% yield. ^{1}H NMR (500 MHz, $CDCl_3$) δ 7.35 (d, *J* = 8.5 Hz, 1H), 6.51(dd, *J* = 2 Hz, 2.5 Hz, 1H), 6.45 (d, *J* = 2.5 Hz, 1H), 5.98 (s, 1H), 4.24 (s, 1H), 3.17 (t, *J* = 7 Hz, 2H), 2.35 (s, 3H), 1.69 - 1.63 (m, 2H), 1.42 - 1.38 (m, 4H), 0.94 (t, *J* = 7 Hz, 3H). ^{13}C NMR (126 MHz, $CDCl_3$) δ 162.0, 156.0, 152.9, 151.7, 125.4, 110.3, 110.2, 109.2, 97.9, 43.4, 29.1, 28.8, 22.4, 18.5, 13.9. HRMS (ESI) m/z calculated for $C_{15}H_{19}O_2N$ $[M + H]^+$ calculated as 245.1416, found 245.1405.

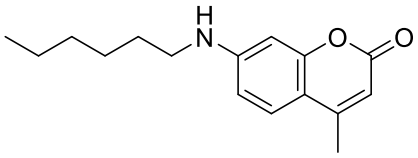

4-methyl-7-(hexylamino)-*2H*-chromen-2-one (13): The representative general procedure mentioned above was followed. The compound was purified by column chromatography using 40% ethyl acetate:hexane. Compound **13** was obtained as a brown solid with 83% yield. ^{1}H NMR (500 MHz, $CDCl_3$) δ 7.36 (d, *J* = 8.5 Hz, 1H), 6.51 (dd, *J* = 2.5 Hz, 2 Hz, 1H), 6.45 (d, *J* = 2.5 Hz, 1H), 5.99 (s, 1H), 4.21 (s, 1H), 3.18 (t, *J* = 7.5 Hz, 2H), 2.36 (s, 3H), 1.69-1.63 (m, 2H), 1.36 - 1.30 (m, 6H), 0.93 (t, *J* = 6.5 Hz, 3H). ^{13}C NMR (126 MHz, $CDCl_3$) δ 161.0, 155.0, 152.0, 150.6, 124.4, 109.3,109.2, 108.2, 96.9, 42.5, 28.6, 28.1, 25.7, 21.5, 17.5, 13.0. HRMS (ESI) m/z calculated for $C_{16}H_{21}O_2N$ $[M + H]^+$ calculated as 260.1645, found 260.1652.

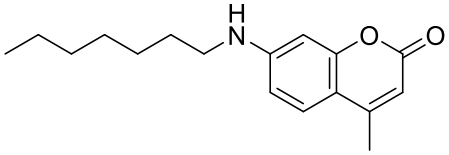

4-methyl-7-(heptylamino)-*2H*-chromen-2-one (14): The representative general procedure mentioned above was followed. The compound was purified by column chromatography using 40% ethyl acetate:hexane. Compound **14** was obtained as a dark brown solid with 84% yield. ^{1}H NMR (600 MHz, $CDCl_3$) δ 7.35 (d, *J* = 9 Hz, 1H), 6.51 (dd, *J* = 2.4 Hz, 1.8 Hz, 1H), 6.44 (d, *J* = 1.8 Hz, 1H), 5.98 (s, 1H), 4.29 (s, 1H), 3.16 (t, *J* = 7.2 Hz, 2H), 2.35 (s, 3H), 1.68 - 1.63 (m, 2H), 1.35 - 1.30 (m, 8H), 0.90 (t, *J* = 6.6 Hz, 3H). ^{13}C NMR (151 MHz, $CDCl_3$) δ 162.1, 156.0, 153.0, 151.7, 125.4, 110.3, 110.2, 109.1, 97.8, 43.5, 31.8, 29.1, 29.0, 27.0, 22.6, 18.5, 14.0. HRMS (ESI) m/z calculated for $C_{17}H_{23}O_2N$ $[M + H]^+$ calculated as 273.1729, found 273.1735.

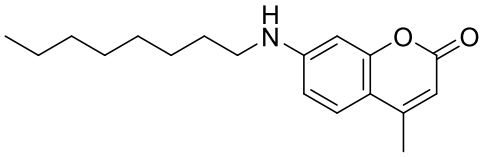

4-methyl-7-(octylamino)-*2H*-chromen-2-one (15): The representative general procedure mentioned above was followed. The compound was purified by column chromatography using 40% ethyl acetate:hexane. Compound **15** was obtained as a dark brown solid with 87% yield.

^{1}H NMR (500 MHz, $CDCl_3$) δ 7.36 (d, *J* = 8.5 Hz, 1H), 6.51 (dd, *J* = 2.5 Hz, 2 Hz, 1H), 6.45 (d, *J* = 2 Hz, 1H), 5.99 (s, 1H), 4.20 (s, 1H), 3.18 (t, *J* = 7 Hz, 2H), 2.36 (s, 3H), 1.69 - 1.63 (m, 2H), 1.45 - 1.39 (m, 2H), 1.35-1.30 (m, 8H), 0.91 (t, *J* = 6.5 Hz, 3H). ^{13}C NMR (126 MHz, $CDCl_3$) δ 162.0, 156.0, 153.0, 151.6, 125.4, 110.4, 110.2, 109.3, 97.9, 43.5, 31.8, 29.3, 29.2, 29.1, 27.0, 22.6, 18.5, 14.1. HRMS (ESI) m/z calculated for $C_{18}H_{25}O_2N$ $[M + H]^+$ as 287.1885, found 287.1893.

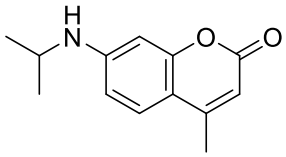

4-methyl-7-(isopropylamino)-*2H*-chromen-2-one (16): The representative general procedure mentioned above was followed. The compound was purified by column chromatography using 40% ethyl acetate:hexane. Compound **16** was obtained as a greenish brown solid with 83% yield. ^{1}H NMR (500 MHz, $CDCl_3$) δ 7.36 (d, *J* = 8.5 Hz, 1H), 6.48 (dd, *J* = 2.5, 2.5 Hz, 1H), 6.45 (d, *J* = 2.5 Hz, 1H), 5.99 (s, 1H), 4.06 (s, 1H), 3.73 - 3.66 (m, 1H), 2.36 (s, 3H), 1.28 (s, 3H), 1.27 (s, 3H). ^{13}C NMR (126 MHz, $CDCl_3$) δ 162.0, 156.0, 152.9, 150.6, 125.5, 110.6, 110.2, 109.2, 98.2, 44.2, 22.7, 18.5. HRMS (ESI) m/z calculated for $C_{13}H_{15}O_2N$ $[M + H]^+$ calculated as 217.1103, found 217.1093.

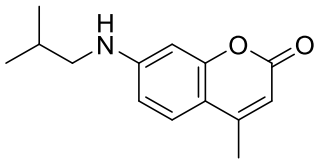

4-methyl-7-(isobutylamino)-*2H*-chromen-2-one (17): The representative general procedure mentioned above was followed. The compound was purified by column chromatography using 30% ethyl acetate:hexane. Compound **17** was obtained as a brownish yellow solid with 82% yield. ^{1}H NMR (500 MHz, $CDCl_3$) δ 7.35 (d, *J* = 9 Hz, 1H), 6.52 (dd, *J* = 2 Hz, 2.5 Hz, 1H), 6.45 (d, *J* = 2 Hz, 1H), 5.98 (s, 1H), 4.31 (s, 1H), 3.01 (d, *J* = 6.5 Hz, 2H), 2.35 (s, 3H), 1.98 - 1.90 (m, 1H), 1.02 (d, *J* = 6.5 Hz, 6H). ^{13}C NMR (126 MHz, $CDCl_3$) δ 162.0, 156.0, 152.9,

151.7, 125.4, 110.3, 110.2, 109.2, 97.9, 51.2, 28.0, 20.3, 18.5. HRMS (ESI) m/z calculated for $C_{14}H_{17}O_2N$ $[M + H]^+$ calculated as 232.1332, found 232.1320.

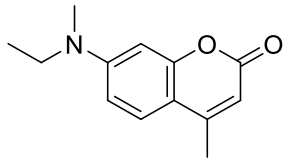

4-methyl-7-(ethyl(methyl)amino)-*2H*-chromen-2-one (18): The representative general procedure mentioned above was followed. The compound was purified by column chromatography using 30% ethyl acetate:hexane. Compound **18** was obtained as a yellow solid with 79% yield.^{1}H NMR (500 MHz, $CDCl_3$) δ 7.37 (d, *J* = 8.5 Hz, 1H), 6.59 (dd, *J* = 2.5 Hz, 2 Hz, 1H), 6.49 (d, *J* = 1.5 Hz, 1H), 5.94 (s, 1H), 3.44 (q, *J* = 7 Hz, 2H), 2.98 (s, 3H), 2.33 (s, 3H), 1.15 (t, *J* = 7.5 Hz, 3H). ^{13}C NMR (126 MHz, $CDCl_3$) δ 162.2, 155.9, 152.9, 151.7, 125.4, 109.4, 109.1, 108.7, 98.1, 46.8, 37.6, 18.5, 11.4. HRMS (ESI) m/z calculated for $C_{13}H_{15}O_2N$ $[M + H]^+$ calculated as 217.1103, found 217.1093.

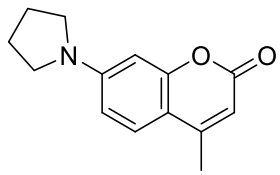

4-methyl-7-(pyrrolidin-1-yl)-*2H*-chromen-2-one (19): The representative general procedure mentioned above was followed. The compound was purified by column chromatography using 30% ethyl acetate:hexane. Compound **19** was obtained as a brown solid with 83% yield. ^{1}H NMR (600 MHz, $CDCl_3$) δ 7.40 (d, *J* = 9.0 Hz, 1H), 6.50 (dd, *J* = 2.4 Hz, 1.8 Hz, 1H), 6.39 (d, *J* = 2.4 Hz, 1H), 5.96 (s, 1H), 3.37 (t, *J* = 6.6 Hz, 4H), 2.36 (s, 3H), 2.08 - 2.06 (m, 4H). ^{13}C NMR (150 MHz, $CDCl_3$) δ 162.3, 155.8, 153.1, 150.3, 125.4, 109.3, 108.9, 108.6, 97.9, 47.7, 29.7, 25.4, 18.5. HRMS (ESI) m/z calculated for $C_{14}H_{15}O_2N$ $[M + H]^+$ calculated as 230.1176, found 230.1197.

4.5. References

(1) Gandioso, A.; Bresolí-Obach, R.; Nin-Hill, A.; Bosch, M.; Palau, M.; Galindo, A.; Contreras, S.; Rovira, A.; Rovira, C.; Nonell, S.; Marchán, V. Redesigning the Coumarin Scaffold into Small Bright Fluorophores with Far-Red to Near-Infrared Emission and Large Stokes Shifts Useful for Cell Imaging. *J. Org. Chem.* **2018**, *83* (3), 1185–1195. https://doi.org/10.1021/acs.joc.7b02660.

(2) Yodoshi, M.; Tani, A.; Ohta, Y.; Suzuki, S. Optimized Conditions for High-Performance Liquid Chromatography Analysis of Oligosaccharides Using 7-Amino-4-Methylcoumarin as a Reductive Amination Reagent. *J. Chromatograph. A* **2008**, *1203* (2), 137–145. https://doi.org/10.1016/j.chroma.2008.07.053.

(3) Rovira, A.; Gandioso, A.; Goñalons, M.; Galindo, A.; Massaguer, A.; Bosch, M.; Marchán, V. Solid-Phase Approaches for Labeling Targeting Peptides with Far-Red Emitting Coumarin Fluorophores. *J. Org. Chem.* **2019**, *84* (4), 1808–1817. https://doi.org/10.1021/acs.joc.8b02624.

(4) Grimm, J. B.; English, B. P.; Chen, J.; Slaughter, J. P.; Zhang, Z.; Revyakin, A.; Patel, R.; Macklin, J. J.; Normanno, D.; Singer, R. H.; Lionnet, T.; Lavis, L. D. A General Method to Improve Fluorophores for Live-Cell and Single-Molecule Microscopy. *Nat. Methods* **2015**, *12* (3), 244–250. https://doi.org/10.1038/nmeth.3256.

(5) Bassolino, G.; Nançoz, C.; Thiel, Z.; Bois, E.; Vauthey, E.; Rivera-Fuentes, P. Photolabile Coumarins with Improved Efficiency through Azetidinyl Substitution. *Chem. Sci.* **2018**, *9* (2), 387–391. https://doi.org/10.1039/C7SC03627B.

(6) Liu, X.; Qiao, Q.; Tian, W.; Liu, W.; Chen, J.; Lang, M. J.; Xu, Z. Aziridinyl Fluorophores Demonstrate Bright Fluorescence and Superior Photostability by Effectively

Inhibiting Twisted Intramolecular Charge Transfer. *J. Am. Chem. Soc.* **2016**, *138* (22), 6960–6963. https://doi.org/10.1021/jacs.6b03924.

(7) Bassolino, G.; Halabi, E.; Rivera-Fuentes, P. Practical and Scalable Synthesis of 7-Azetidin-1-Yl-4-(Hydroxy-methyl)Coumarin: An Improved Photoremovable Group. *Synthesis* **2018**, *50* (04), 846–852. https://doi.org/10.1055/s-0036-1591742.

(8) Denmark, S. E.; Sweis, R. F. Cross-Coupling Reactions of Alkenylsilanols with Fluoroalkylsulfonates. *Org. Lett.* **2002**, *4* (21), 3771–3774. https://doi.org/10.1021/ol026900x.

(9) Uemura, M.; Yorimitsu, H.; Oshima, K. Cp∗Li as a Base: Application to Palladium-Catalyzed Cross-Coupling Reaction of Aryl-X or Alkenyl-X (X=I, Br, OTf, ONf) with Terminal Acetylenes. *Tetrahedron* **2008**, *64* (8), 1829–1833. https://doi.org/10.1016/j.tet.2007.11.095.

(10) Anderson, K. W.; Mendez-Perez, M.; Priego, J.; Buchwald, S. L. Palladium-Catalyzed Amination of Aryl Nonaflates. *J. Org. Chem.* **2003**, *68* (25), 9563–9573. https://doi.org/10.1021/jo034962a.

(11) Högermeier, J.; Reissig, H.-U. Nine Times Fluoride Can Be Good for Your Syntheses. Not Just Cheaper: Nonafluorobutanesulfonates as Intermediates for Transition Metal-Catalyzed Reactions. *Adv. Synth. Catal.* **2009**, *351* (17), 2747–2763. https://doi.org/10.1002/adsc.200900566.